HEPCAT Progress Report: SiPM and Materials R&D for Current and Future Dark Matter Detectors

Aras Repond; University of California, Riverside, CA

October 6th, 2025

1 Introduction

DarkSide-20k is a direct detection experiment designed to search for weakly interacting massive particles (WIMPs), one of the leading candidates for dark matter. While WIMPs are hypothetical particles that will interact very rarely with ordinary matter, they may produce faint signals that detectors like Darkside-20k are built to measure.

Detecting such rare interactions requires highly sensitive light sensors. For this reason, DarkSide-20k employs silicon photomultipliers (SiPMs) throughout the main detector as well as in the outer veto system, which surrounds the time projection chamber (TPC). In both locations, SiPMs are responsible for detecting the tiny flashes of light produced by particle interactions in the liquid argon, enabling the identification of potential dark matter events.

The SiPM R&D conducted at the University of California Riverside focuses on informing the design of the next generation of DarkSide detectors. One of these detectors is DarkSide-LowMass, which will focus on an S2-only search, meaning that it will rely solely on secondary scintillation signals produced when ionization electrons are drifted and extracted into the gas phase, rather than using the primary scintillation (S1) signals. Because of this, the readout system must achieve a large dynamic range while maintaining high gain. The goal is to be sensitive to sub-keV dark matter signals while also detecting MeV-scale gamma rays for calibration, ensuring accurate characterization across a broad energy range. To meet these requirements, work at UCR is addressing how best to accommodate this large dynamic range while also optimizing readout board gain, minimizing noise, and developing effective channel summing strategies. Although this R&D will be too late to influence DarkSide-20k directly, it will provide valuable input for design decisions in future detectors.

The outer veto system further enhances the Darkside-20k detector's performance. Its inner walls will be lined with reflective material to maximize light collection, and SiPMs will be attached to the outside of the TPC to optimize photon detection. These design elements increase overall light detection efficiency, allowing the system to discriminate between backgrounds and true ionizing radiation events, while maintaining sensitivity to any unusual signals that could indicate interesting new physics.

2 SiPM Research and Development

2.1 SiPM Setup

The SiPMs I have chosen to begin my R&D with are the Hamamatsu S14161-6050HS-04, which consists of an array of sixteen SiPMs arranged in a 4×4 configuration. Each channel has an effective photosensitive area of 6.0×6.0 mm^2, with a broad spectral response ranging from 270nm to 900nm. To read out signals from these SiPMs, I started with a prototype readout board schematic provided by AstroCeNT and had a Chinese manufacturer (JLCPCB) produce five boards, two fully populated and three unpopulated. I have primarily been testing one of the populated boards (Figure 1), with plans to populate one of the unpopulated boards myself to verify that I can replicate the same production quality achieved by JLCPCB. After using a reflow oven to attach the SiPM array (Figure 2), the board was ready to begin reading out signals, allowing me to start the characterization processes necessary for the R&D effort.

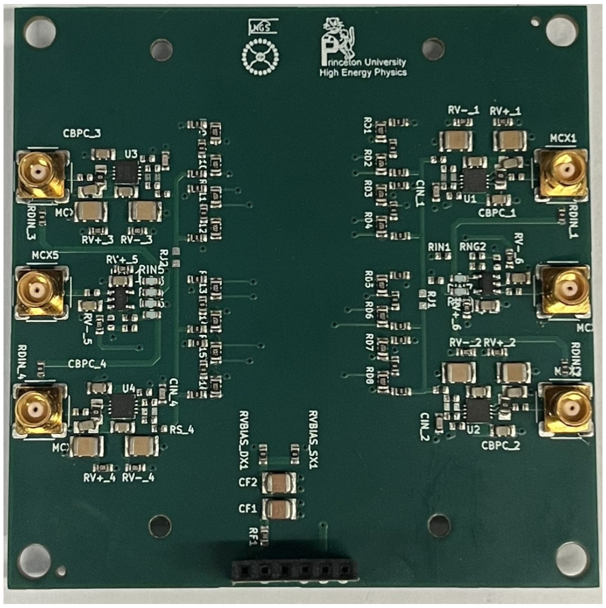

Figure 1: Back side of Readout Board

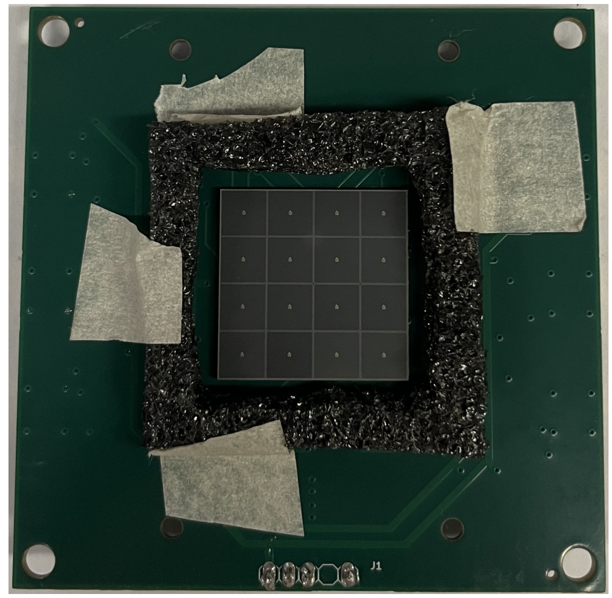

Figure 2: Front side of Readout Board with Foam Protector

The data acquisition setup consists of a custom-built dark box, a Picoscope 3406D oscilloscope, a CAEN SY5527 primary high-voltage power supply, and a Siglent SPD3303X-E programmable DC power supply. Cryogenic measurements were performed by positioning the readout board above a container of liquid nitrogen, allowing signals to be recorded at low temperatures.

2.2 Python Analysis

The initial waveforms revealed that signal processing is essential before meaningful analysis can be performed. The first step is baseline subtraction, where the average of the first 20% of the waveform is calculated and subtracted uniformly from all data points. Next, the signal is smoothed using a rolling integral implemented as a moving average filter of length 7, applied iteratively 7 times. The choice of 7 was determined through trial and error, as it provided the best balance between noise reduction and signal preservation. Finally, peaks are identified using SciPy's find_peaks algorithm. For each detected peak, both the height and the integral are extracted, which are then used to construct finger plots based on the amplitude and charge of individual pulses [1].

2.3 Characterization

Characterization of the SiPMs started with the analysis of dark data. The initial focus was on studying how overvoltage, the difference between breakdown voltage and bias voltage, impacts the signal quality. At room temperature, higher overvoltages (3 VoV) produced cleaner signals, while at cryogenic temperatures the optimal operating point shifted to lower overvoltages (1–2 VoV). These effects are particularly impactful when it comes to analyzing dark data, because trapped carriers take much longer to release at lower temperatures, which increases noise from afterpulsing and cross talk effects when at higher overvoltages.

Generating finger plots at room temperature has proved challenging, requiring stringent data cuts to isolate clean pulses. This effort is still ongoing, and producing clear warm finger plots remains a priority. In comparison, the cryogenic finger plots exhibit well-defined and easily distinguishable photoelectron (PE) peaks, as illustrated in Figures 3 and 4, where both the amplitude and charge have been used to identify the first five PE peaks. The linearity of these plots, shown in Figures 5 and 6, is particularly important because it verifies that the SiPM response scales proportionally with the number of detected photons, confirming the reliability of both amplitude and charge based analysis methods. This linearity is essential for accurate calibration, precise gain measurements, and the interpretation of low-energy signals in future dark matter searches.

From the cryogenic dataset, an average single-photoelectron (SPE) pulse was produced by selecting high-quality pulses, aligning them at the peak, and averaging over approximately 3,000 events, yielding Figure 7. The resulting average pulse has a sharp, fast rise time followed by a small, persistent "bump" approximately 80ns after the initial peak. Although this small bump is unusual, it is likely caused by parasitic capacitances in the feedback loop of the amplifier. Fitting this averaged waveform using the sum of a gaussian and an exponential decay (Equation 1) results in a decay time constant of 0.1044 ± 0.0429 μs (table 1), which is consistent with expected SiPM pulse characteristics at cryogenic temperatures, indicating that the readout and analysis are performing as intended.

$$f(t) = A \cdot \exp\left(-\frac{(t-\mu)^2}{2\sigma^2}\right) + C + \begin{cases} B \cdot \exp\left(-\frac{t-\mu}{\tau}\right), & t \geq \mu \\ 0, & t < \mu \end{cases} \tag{1}$$

Parameter	Value
A (mV)	-0.6114 ± 0.01724
μ (μs)	0.245 ± 0.001765
σ (μs)	0.01409 ± 0.001745
B (mV)	-0.1989 ± 0.06301
τ (μs)	0.1044 ± 0.04287
C (mV)	0.005415 ± 0.01277

Table 1: Fit results from Figure 7.

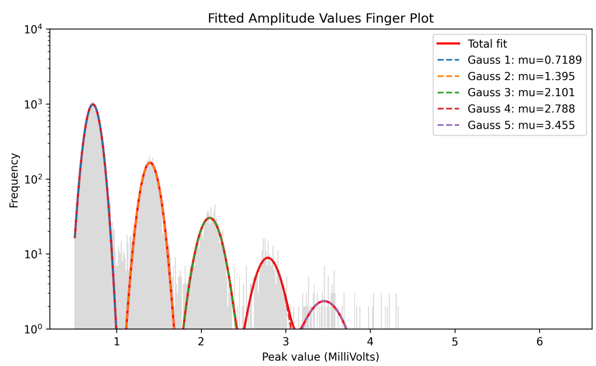

Figure 3: Amplitude fit

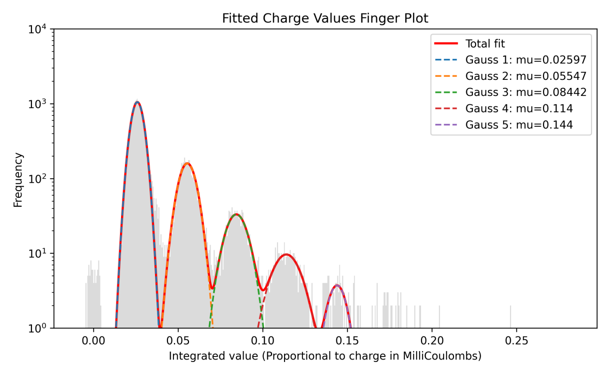

Figure 4: Charge fit

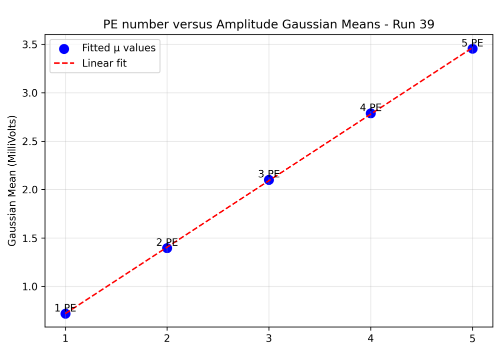

Figure 5: Amplitude linearity

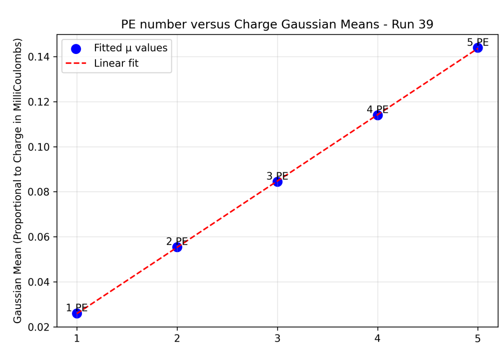

Figure 6: Charge linearity

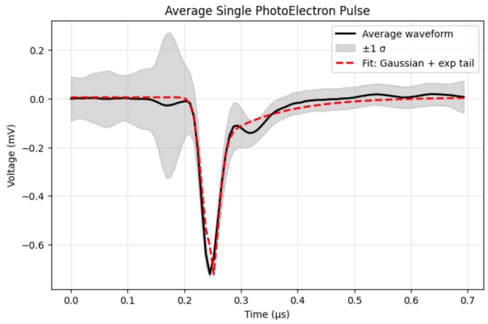

Figure 7: Average SPE Pulse with Fit

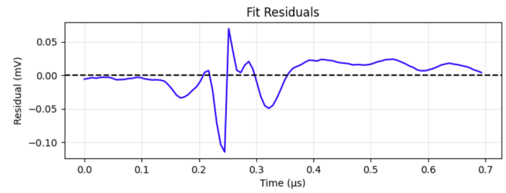

Figure 8: Average SPE Pulse Fit Residuals

3 Simulation and Modeling of Parasitic Effects

To better understand the behavior of the readout board, KiCad SPICE simulations were performed to investigate the effects of parasitic capacitances in the feedback loop of the transimpedance amplifier (TIA). In these simulations, the SiPM was modeled as a current source in parallel with a capacitor, which accounts for the intrinsic output capacitance of the device. The TIA then converts this SiPM current pulse into a voltage pulse, with the feedback resistor setting the transimpedance gain. For the prototype AstroCeNT board schematic, a 10 kΩ feedback resistor is used, and no explicit feedback capacitor is included. These simulations (Figure 9) were compared to real measurements, capturing the slight "ringing" that can be seen in the averaged single-photoelectron pulse (Figure 7).

It is theorized that the observed ringing arises from parasitic capacitances in the feedback loop, which, in combination with the feedback resistor, create an underdamped oscillator. In this configuration, the fast rising edge of the SiPM current pulse excites the loop, producing a small oscillatory voltage response before settling to the baseline.

Using the SPICE model, it was found that increasing the feedback capacitance can mitigate this underdamped behavior. The nominal parasitic capacitance of approximately 2 pF, primarily arising from PCB trace layout, produces noticeable ringing. By adding a 1pF feedback capacitor, which was determined through trial-and-error simulations, the response of the TIA becomes critically damped, resulting in a cleaner voltage pulse (Figure 10).

The next step is to implement this increased feedback capacitance on the actual readout board and verify whether the bump or ringing in the averaged waveform is eliminated, thereby improving the accuracy of the SiPM signal readout.

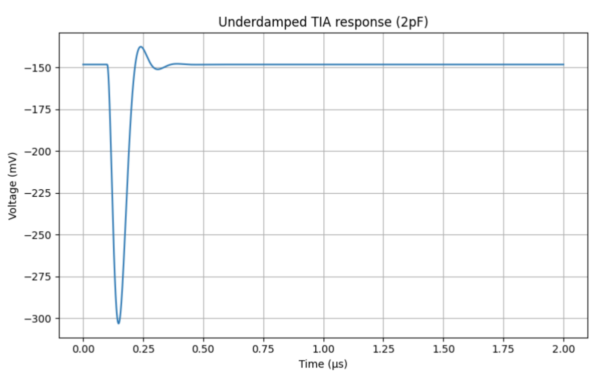

Figure 9: Underdamped TIA Response

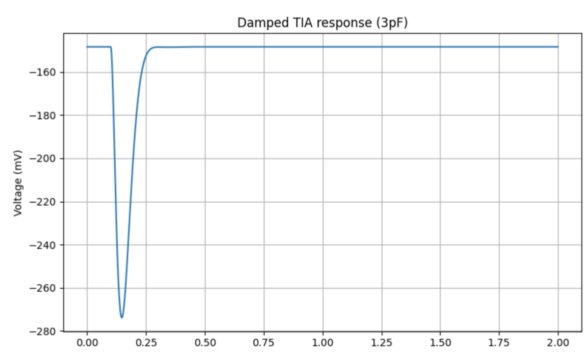

Figure 10: Damped TIA Response

3.1 Future Plans

My next steps for SiPM analysis build directly on the knowledge I have gained from characterizing the AstroCeNT readout board. The immediate goal is to develop the next prototype and use it to test different feedback resistor and capacitor values, optimizing the SiPM response in terms of gain, noise, and bandwidth. I also plan to explore the trade-offs between summing multiple channels versus a single-channel readout scheme. Extending this work to SiPMs from different manufacturers will allow me to fine-tune the amplification network for each individual device, ensuring optimal performance across a variety of SiPM models.

To make this process more efficient, I am proposing a dual-board design. In this configuration, a front-end board would hold the SiPM array, while a back-end board would handle biasing, amplification, and channel summing. This "plug-and-play" design will make it possible to rapidly swap boards for testing without extensive soldering.

On the analysis side, I plan to develop software to automate IV curve measurements, generate finger plots, control bias voltage levels, and measure dark count rates (DCR). Current plans are to interface with MIDAS, which is a data acquisition software developed at TRIUMF [2]and used in the lab here at UCR.

Finally, I aim to verify that I can replicate the same production quality as JLCPCB. This will be accomplished using the reflow oven and SMT Caddy (manual pick-and-place machine) available in the ECE MakeRSpace at UCR, giving me hands-on experience in building SiPM readout hardware.

4 Lumirror Tests

4.1 Cryogenic Lumirror Stress Test

The reflective material under consideration for lining the cryostat walls is Lumirror, a biaxially oriented polyester film. Maintaining the mechanical integrity of this reflector is critical for the long-term stability of the DarkSide-20k experiment; and so to verify the cryogenic stability of Lumirror, experiments have been conducted at UCR.

Using a FLUKA simulation performed by Kevin Thieme (University of Hawai'i at Mānoa) [3], the maximum force on the reflector during cryogenic operation is predicted to be approximately 10 N/m^2. Given that our Lumirror rolls measure 8 m × 1 m, this corresponds to a total force of roughly 80 N per roll. With six attachment points available (constrained by the cryostat geometry), this yields an estimated 13.3 N per attachment point.

To test this experimentally, a small sample was mounted with two attachment points and subjected to a load of approximately 2.7 kg (26.6 N) while submerged in liquid nitrogen for 40 hours. In the initial setup, holes were punched in the Lumirror, and bolts were used to suspend the sample (Figure 11). This resulted in minor damage around the attachment points. To address this, tests are now being repeated using grommets to reinforce each attachment point. These tests are ongoing, with the goal of completing them within the next year.

4.2 Room Temperature Lumirror Stress Test

In addition to testing Lumirror at cryogenic temperatures, it is also important to evaluate its durability at room temperature. The geometry of the cryostat presents a unique engineering challenge, as attachment points are only available at the corners, approximately 8 meters apart. To simulate this, test stands were constructed with attachment points positioned 340 mm apart vertically, mimicking the relative orientation in the actual cryostat. By suspending an 8 m × 1 m roll of Lumirror from these stands, we were able to replicate how the material will hang under real conditions (Figure 12). Initial tests using a hole punch and washer attachment method resulted in small tears in the material, which prompted ongoing tests with reinforced grommets to improve durability. Again, I aim to complete these tests and finalize the attachment design in the next year.

5 Italy Trip to LNGS Summer 2025

The last highlight I'd like to share from this past year is the two months I spent working in Italy at Laboratori Nazionali del Gran Sasso – INFN (LNGS), supported by HEPCAT travel funds. While there, I was able to contribute to the photo-detector unit (PDU) assembly process for DarkSide-20k, which gave me valuable hands-on experience handling sensitive Fondazione Bruno Kessler (FBK) SiPMs developed specifically for the DS20K experiment. I also assisted with quality assurance and quality control testing of the SiPM tiles

Figure 11: Cryogenic Lumirror Stress Test

Figure 12: Room Temperature Lumirror Stress Test

before their integration into the PDUs, and gained firsthand experience with large-scale detector assembly procedures.

6 Conclusion

Throughout the past year, I have been given the chance to build both technical skills and hands-on experience that will directly support my contributions to current and future Darkside experiments. From developing a deeper understanding of detector assembly procedures at LNGS to working with SiPM testing and analysis, I've been able to connect the R&D completed here at UCR to the larger goals of the Darkside collaboration. I'm grateful for the financial support I've received through the HEPCAT fellowship, and I'm excited to continue my research in the upcoming year.

References

[1] Repondaras. (n.d.). *SiPM-python-analysis*. GitHub. Retrieved October 2, 2025, from `https://github.com/repondaras/SiPM-python-analysis`

[2] TRIUMF. (n.d.). *Main page*. MidasWiki. Retrieved October 2, 2025, from `https://daq00.triumf.ca/MidasWiki/index.php/Main_Page`

[3] Thieme, K. (2023). *Outer veto CFD*. In *Proceedings of the 2023 INFN Workshop on Advanced Detector Technologies* (pp. 1–10). Retrieved October 2, 2025, from `https://agenda.infn.it/event/33431/contributions/184621/attachments/99099/137340/Outer_Veto_CFD_Kevin_Thieme.pdf`